

# Measurement of small vibration amplitudes of a rough surface by an interferometer with a self-pumped phase-conjugate mirror

Xiangzhao Wang, Osami Sasaki, Takamasa Suzuki, and Takeo Maruyama

The application of a Michelson interferometer with a self-pumped phase-conjugate mirror to measure small vibration amplitudes of a rough surface is described. The distorted wave front of the light that is diffusely reflected from the rough surface is restored by phase conjugation to provide an interference signal with a high signal-to-noise ratio. The vibration amplitudes of a stainless-steel sample are measured with a precision of  $\sim 5$  nm. © 2000 Optical Society of America

OCIS codes: 120.3180, 190.5040, 120.7280.

## 1. Introduction

Interferometers that contain phase-conjugate mirrors (PCM's) have been intensively researched. As an element of an interferometer the PCM has many advantages such as self-alignment, structural simplicity, and a twofold improvement in sensitivity.<sup>1-3</sup> In addition, the PCM can compensate for wave-front distortion of a beam. This property of the PCM was used to compensate automatically for atmospheric turbulence, and the need to place the interferometer arms in vacuum was eliminated.<sup>4</sup> In an interferometric fiber-optic sensor a PCM corrected the distortion that is due to mode scrambling in a multimode fiber.<sup>5</sup> The PCM was also used for removing the aberrations of a diverging beam of light introduced by a beam splitter, and a compensating plate to eliminate the aberrations was not required.<sup>6,7</sup>

Another important application of the distortion-compensation property of a PCM lies in reducing the speckles in the light reflected diffusely by a rough surface to yield interference signals with high signal-to-noise ratio.<sup>8-10</sup> The spatial phase distribution of a wave incident upon a self-pumped phase-conjugate

mirror (SPPCM) is reversed in sign by the SPPCM to generate a self-pumped phase-conjugate wave (SPPCW). When the phase of the incident wave changes because of the time-varying optical path length, the phase change is not reversed in sign but is preserved in the SPPCW because the period of grating formation in the SPPCM is slower than the time-varying phase change. This preservation occurs whether the phase changes are spatially uniform<sup>4,11</sup> or nonuniform.<sup>12,13</sup> Therefore the phase changes caused by vibrations of a rough surface are preserved in the SPPCW. The vibration amplitudes of the rough surface can be measured exactly by interference between the SPPCW and a reference wave.

In this paper we report on our measurements of the distributions of the vibration amplitude of a rough surface by using a SPPCM. The wave-front distortion of the light reflected from the rough surface is compensated for by the SPPCM. When spatially uniform phase changes occur in the incident wave, the reflectivity of the SPPCM does not change. The vibrations of a rough-surface object, however, cause a spatial nonuniformity of the phase changes. This nonuniformity causes a corresponding decrease in the reflectivity of the SPPCM.<sup>12,13</sup> When the vibration amplitudes of the rough-surface object are larger than  $\sim 500$  nm, the reflectivity of the SPPCM will decrease nearly to zero in many places because of large deformations of the rough surface. We measure vibration amplitudes of a rough surface that are less than  $\sim 200$  nm, so the reduction in reflectivity of the SPPCM has no influence on the measurements of the vibration amplitudes.

In Section 2 we describe the measurement, with an

O. Sasaki (osami@eng.niigata-u.ac.jp), T. Suzuki, and T. Maruyama are with the Faculty of Engineering, Niigata University, Niigata 950-2181, Japan. X. Wang is with the Shanghai Institute of Optics and Fine Mechanics, Chinese Academy of Sciences, Shanghai 201800, China.

Received 18 January 2000; revised manuscript received 17 May 2000.

0003-6935/00/254593-05\$15.00/0

© 2000 Optical Society of America

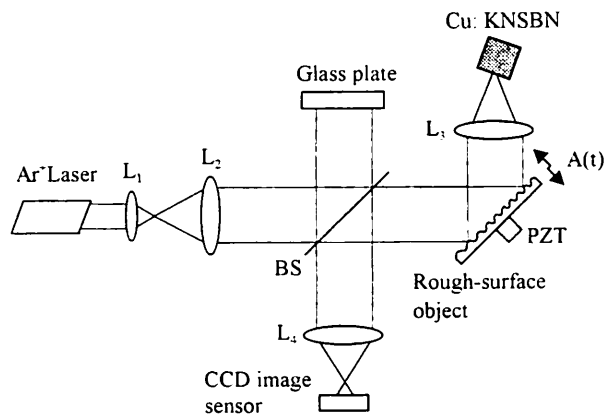


Fig. 1. Michelson interferometer with a SPPCM used for measurements of the vibration-amplitude distributions of a rough-surface object: L, lens; BS, beam splitter; PZT, piezoelectric transducer; Cu:KNSBN, Cu-doped KNSBN crystal.

interferometer with a SPPCM, of vibration amplitudes of a rough surface. The experimental results of measurements of the rough surface of a stainless-steel sample are presented in Section 3 below.

## 2. Interferometer

Figure 1 shows a Michelson interferometer with a SPPCM in one arm. We use it to measure vibration amplitudes of a rough-surface object. A laser beam expanded and collimated with lenses  $L_1$  and  $L_2$ , respectively, is directed by beam splitter BS onto a glass plate and to a rough-surface object that is sinusoidally vibrated by a piezoelectric transducer (PZT). The light reflected diffusely from the rough surface is gathered onto a SPPCM by lens  $L_3$ . A phase-conjugate wave of the incident light produced by the SPPCM returns to the rough surface by the same path. After the second reflection from the rough surface, the light, whose wave front is now distorted, is again a plane wave. This plane wave interferes with the reference wave reflected by the glass plate. The interference signal is detected by a two-dimensional CCD image sensor.

The vibration of point  $P(x, y)$  on the rough surface is represented by

$$A(x, y, t) = a(x, y)\cos(\omega_c t), \quad (1)$$

and the direction of the vibration is nearly normal to the plane of the rough surface. Point  $P(x, y)$  moves to position Q as a result of the vibration when  $A = a$ , as shown in Fig. 2, where  $\gamma$  is the angle between the ray of light incident upon the rough surface and the direction of the vibration. A detection point  $(x', y')$  on the CCD image sensor receives the phase-conjugate light beam reflected at point P when  $A = 0$ . During the vibration the points that exist between R and S send the light beams to the detection point  $(x', y')$ . These points on the surface are called sampling points for detection point  $(x', y')$ . The vibration amplitude is assumed to be constant over the sampling points, and the surface between R and S is assumed

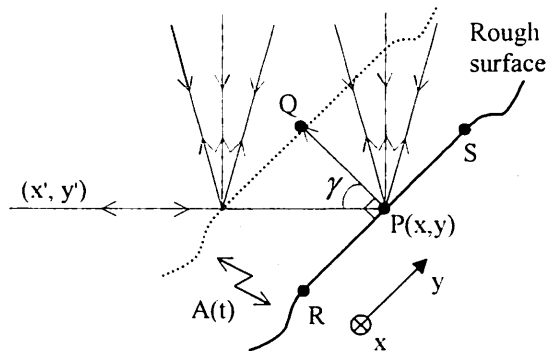


Fig. 2. Sheet of stainless steel used as the rough-surface object.

to be a plane, which means that the correlation distance of the rough surface is much longer than the distance between points R and S. These assumptions hold because the region where the sampling points are located is small when the vibration amplitude is less than 200 nm and angle  $\gamma$  is  $\sim 45$  deg. The change in the optical path of the ray of light that falls upon the sampling points is  $A(x, y, t)/\cos \gamma$ . The phase change of the wave incident that is upon the SPPCM is given by

$$\Delta\alpha(x, y, t) = (2\pi/\lambda)[a(x, y)/(\cos \gamma)]\cos(\omega_c t), \quad (2)$$

where  $\lambda$  is the wavelength of the light. The SPPCM has a phase diffraction grating formed by the incident wave at  $A = 0$ . Time-varying phase change  $\Delta\alpha$  is not reversed in sign by the SPPCM and is preserved in the SPPCW, whose spatial phase distribution does not change during the vibration. Therefore the phase change in the SPPCW at detection point  $(x', y')$  becomes  $2\Delta\alpha$  after the second reflection from the rough surface. The interference intensity at detection point  $(x', y')$  can be expressed as

$$I(x', y', t) = I_0(x', y') + S_0(x', y') \times \cos[Z(x', y')\cos(\omega_c t) + \alpha], \quad (3)$$

where

$$Z(x', y') = (4\pi/\lambda)[a(x', y')/(\cos \gamma)] \quad (4)$$

and  $\alpha$  is a constant.  $I_0$  is a component that is independent of time, and  $S_0$  is the amplitude of the time-varying component.  $I_0$  and  $S_0$  are functions of coordinate  $(x', y')$  relative to the spatial reflectivity distribution of the SPPCM. This is so because the vibrations of the object are accompanied by a spatially nonuniform deformation of the rough surface, which causes a reduction in the reflectivity of the SPPCM. The CCD image sensor detects the interference intensity that involves integration of Eq. (3) over a photodiode element. However, amplitude  $a$  and phase  $\alpha$  of the SPPCW are constant over the photodiode element. Therefore the interference signal detected with the CCD image sensor is represented by Eq. (3), and we can obtain the vibration-amplitude distribution  $a(x, y)$  of the rough-surface

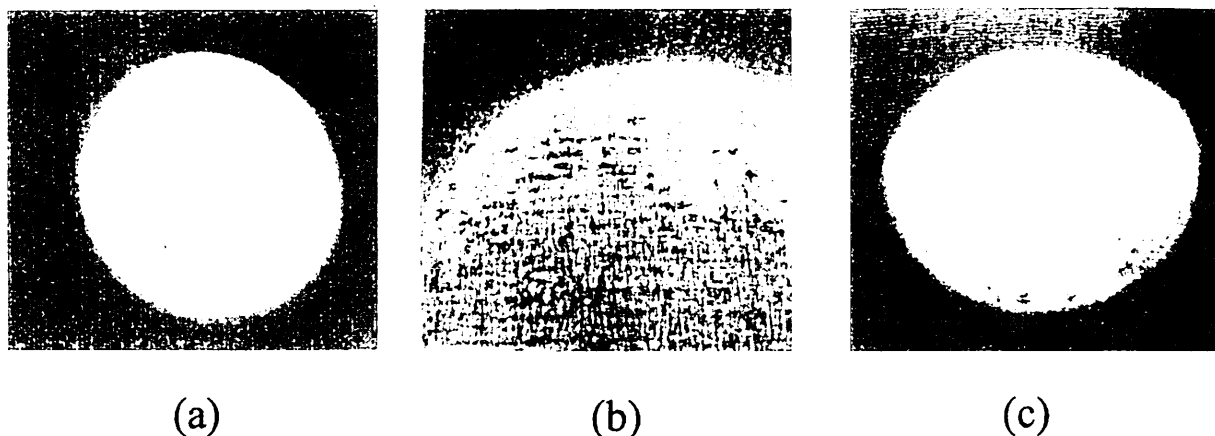


Fig. 3. (a) Gaussian beam, (b) light reflected by the stainless-steel plate, (c) phase-compensated phase-conjugate beam.

object by calculating  $Z$  values with the Fourier-transform method described in Ref. 14.

### 3. Experiments

The experimental setup is shown in Fig. 1. The light source was a single-mode  $\text{Ar}^+$  laser operating at  $\lambda = 514$  nm with a power of  $\sim 90$  mW. Its output was expanded by  $60\times$  microscopic objective lens  $L_1$  and lens  $L_2$  with a focal length of 200 mm into a 35-mm-diameter beam. A stainless-steel plate with a size of  $40$  mm  $\times$   $30$  mm  $\times$   $0.2$  mm thick was used as the rough-surface object. One edge of the object along the  $y$  axis was fixed. A PZT was attached to the rear face of the object, near its central point. The position of the PZT on the surface is called the forced point. The PZT was excited by a sinusoidal voltage  $V(t) = V_a \cos \omega t$ . The vibration direction of the object formed an angle of  $45^\circ$  with the incident beam ( $\gamma = 45^\circ$ ). The light from a Gaussian beam incident upon the object is shown in Fig. 3(a). Figure 3(b) shows the speckle pattern of the light reflected by the object surface. The beam reflected from the object surface was focused by lens  $L_3$ , which had a 45-mm diameter and a 100-mm focal length, onto a Cu:KNSBN crystal. The size of the Cu:KNSBN crystal was  $5.5$  mm  $\times$   $5.7$  mm  $\times$   $7.0$  mm. Its  $c$  axis was parallel to the 7-mm side. The focused beam was incident upon the crystal at an angle of  $60^\circ$  relative to the crystal's  $c$  axis. The beam diameter at the entrance to the crystal was 2 mm. The crystal produced a phase-conjugate wave. When it was reflected by the object surface, the phase-conjugate wave became a Gaussian light beam, which is shown in Fig. 3(c). The distorted wave front shown in Fig. 3(b) was restored by optical phase conjugation. The phase-conjugate reflectivity of the crystal was  $\sim 30\%$  when no voltage was applied to the PZT. To get comparatively high visibility of the interference fringe in the measuring range of the vibration amplitude of the object, we chose a reflectivity of  $\sim 6\%$  for the glass plate. Lens  $L_4$  made an image of the object surface on a CCD image sensor. The interference signal was detected with the CCD image sensor with

$20 \times 20$  photodiode elements. The object surface was at an angle of  $90^\circ - \gamma = 45^\circ$  to the ray of light incident upon it; hence the measured region in the object surface had a rectangular shape. The measured region was  $15$  mm  $\times$   $10$  mm. The output signal of the CCD image sensor was converted from analog to digital and processed in a computer.

Applying the sinusoidal voltage  $V(t)$  to the PZT, we measured the vibration-amplitude distribution  $a(x, y)$  of the object. The measured result at  $V_a = 2.7$  V and  $\omega_c/2\pi = 80$  Hz is shown in Fig. 4. The coordinates of the  $x$  and  $y$  axes are the numbers of photodiode elements of the CCD image sensor. The forced point was at  $x = 12$  and  $y = 10$ . The vibration-amplitude distributions along the lines  $y = 10$  and  $x = 10$  are shown in Figs. 5(a) and 5(b), respectively. Figure 5(a) shows that the vibration amplitude decreases rapidly as it approaches the fixed edge along the  $y$  axis. Figure 5(b) shows that the vibration amplitude is almost constant along the  $y$  axis. At  $V_a = 2.7$  V the vibration amplitude is not large at the forced point. Increasing the amplitude  $V_a$  of the sinusoidal voltage to 3.2 V yielded the amplitude distribution shown in Fig. 6. Here the vibration

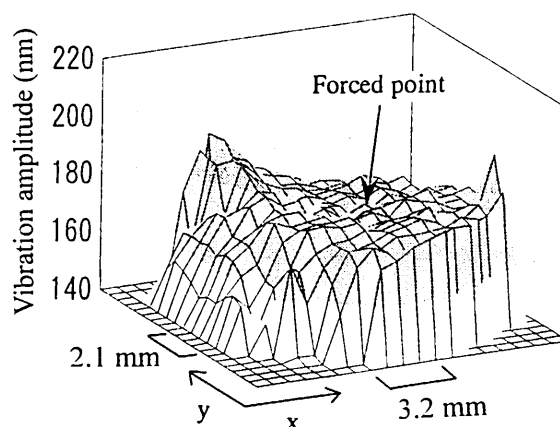
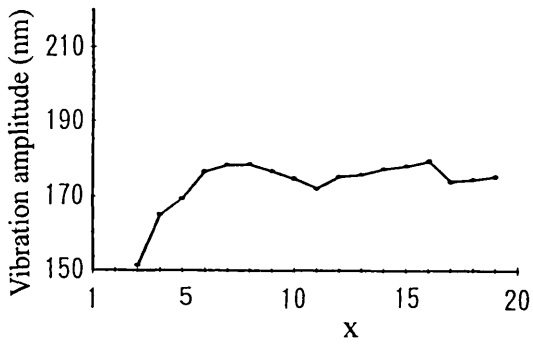
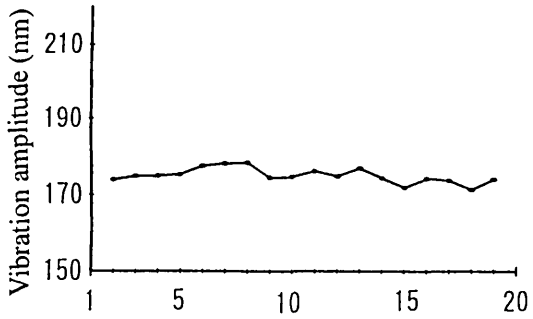


Fig. 4. Vibration-amplitude distribution measured with amplitude of the sinusoidal voltage  $V_a = 2.7$  V.



(a)



(b)

Fig. 5. Vibration-amplitude distributions directed toward (a) the  $x$  axis and (b) the  $y$  axis, taken from Fig. 4.

amplitudes about the forced point are larger than for Fig. 5.

Figure 7 shows phase distributions of a phase-conjugate wave measured under the conditions described above. The phase distribution of the phase-conjugate wave did not change after the amplitude of the object increased. It is clearly shown that the wave front distorted by the rough surface has been restored. Covering the glass plate in Fig. 1 with black paper, we detected intensity distributions of the

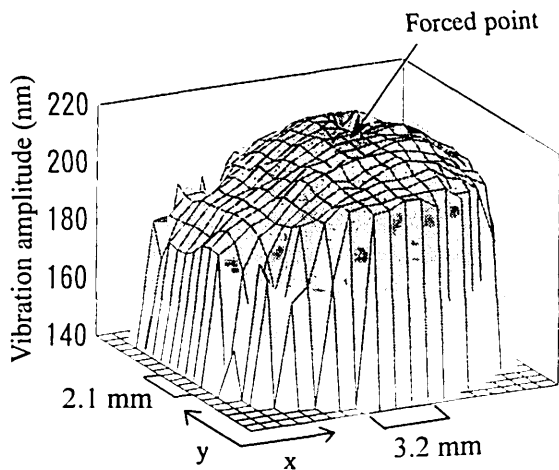
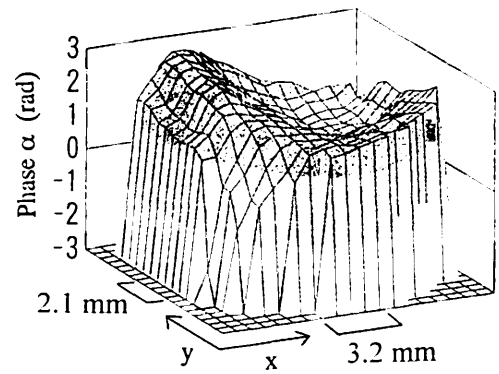
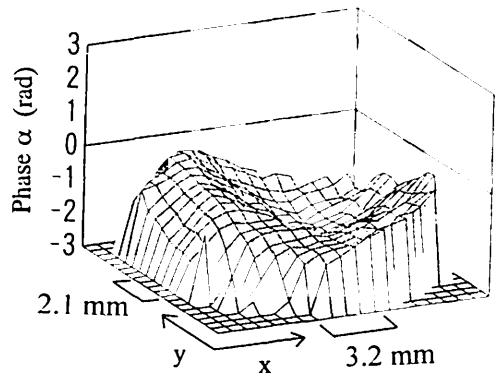


Fig. 6. Vibration-amplitude distribution measured with  $V_a = 3.2$  V.



(a)



(b)

Fig. 7. Phase distributions of the phase-conjugate wave measured at (a)  $V_a = 2.7$  V and (b)  $V_a = 3.2$  V.

phase-conjugate wave. Figure 8 shows the intensity of the phase-conjugate wave at  $V_a = 4$  V relative to that at  $V_a = 0$  V. The relative intensity of the phase-conjugate wave reflects the degree of deformation of the object surface, which is related to the distribution of the vibration amplitude shown in Fig. 6. The remarkable decrease in the vibration amplitude near point A indicated in Fig. 6 caused a large deformation of the object surface. This deformation resulted in a marked decrease of the intensity of the phase-

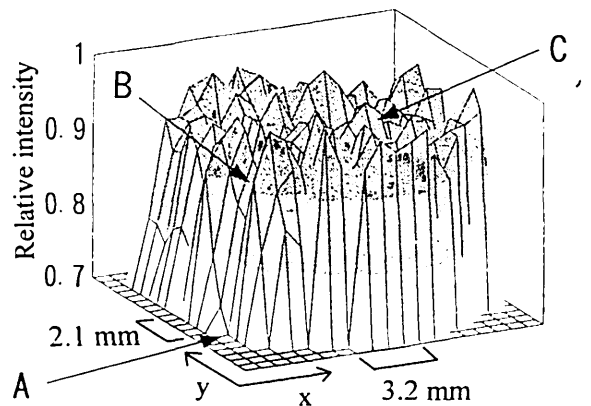


Fig. 8. Relative intensities of the phase-conjugate wave.

conjugate wave at point A, as shown in Fig. 8. As there was scarcely any deformation about point C, as shown in Fig. 6, the relative intensity of the phase-conjugate wave was high. At point B there was a small amount of deformation and a small decrease in the intensity of the phase-conjugate wave. The measurements of the vibration amplitude were repeatable for  $\sim 5$  nm, even when the relative intensity of the phase-conjugate wave was  $\sim 0.7$ .

#### 4. Conclusions

A new method for measuring the vibration-amplitude distribution of a rough-surface object by use of an interferometer with a self-pumped phase-conjugate mirror has been proposed. The distorted wave front of the object wave reflected from the rough surface is restored by use of a phase-conjugate wave to produce an interference signal with a high signal-to-noise ratio. When the vibration amplitudes of the rough surface change, the phase distribution of the phase-conjugate wave does not change, whereas the wave's intensity decreases proportionally to the deformation of the rough surface. The intensity reduction of the phase-conjugate wave has no obvious influence on the measurement of vibration amplitudes of less than 200 nm. The measurements of the vibration amplitude of the rough surface were repeatable for  $\sim 5$  nm.

#### References

1. W. L. Howes, "Large aperture interferometer with a phase-conjugate self-reference beam," *Appl. Opt.* **25**, 3167-3170 (1986).
2. D. J. Gauthier, R. W. Boyd, R. K. Jungquist, J. B. Lisson, and L. L. Voci, "Phase-conjugate Fizeau interferometer," *Opt. Lett.* **14**, 323-325 (1989).
3. X. Wang, O. Sasaki, Y. Takebayashi, T. Suzuki, and T. Maruyama, "Sinusoidal phase-modulating Fizeau interferometer using a self-pumped phase conjugator for surface profile measurements," *Opt. Eng.* **33**, 2670-2674 (1994).
4. J. Feinberg, "Interferometer with a self-pumped phase-conjugating mirror," *Opt. Lett.* **8**, 569-571 (1983).
5. N. S. K. Kwong, "Fiber-optic sensor using a tandem combination of a multimode fiber and a self-pumped phase conjugator," *Opt. Lett.* **14**, 590-592 (1989).
6. R. P. Shukla, M. Dokhanian, P. Venkateswarlu, and M. C. George, "Phase conjugate Twyman-Green interferometer for testing conicoidal surfaces," in *Optical Testing and Metrology III: Recent Advances in Industrial Optical Inspection*, C. P. Grover, ed., Proc. SPIE **1332**, 274-286 (1990).
7. R. P. Shukla, M. Dokhanian, P. Venkateswarlu, and M. C. George, "Phase conjugate Twyman-Green interferometer for testing spherical surfaces and lenses and for measuring refractive indices of liquids or solid transparent materials," *Opt. Commun.* **78**, 407-415 (1990).
8. M. Paul, B. Betz, and W. Arnold, "Interferometric detection of ultrasound at rough surfaces using optical phase conjugation," *Appl. Phys. Lett.* **50**, 1569-1571 (1987).
9. Y. Matsuda, H. Nakano, and S. Nagai, "Optical detection of transient Lamb waves on rough surfaces by a phase-conjugate method," *Jpn. J. Appl. Phys.* **31**, L987-L989 (1992).
10. M. Zhao and I. Yamaguchi, "Self-pumped phase conjugation of diffusely reflected light in a KNSBN crystal," *Opt. Lett.* **20**, 1098-1100 (1995).
11. Y. Tomita, R. Yahalom, and A. Yariv, "Phase shift and cross talk of a self-pumped phase-conjugate mirror," *Opt. Commun.* **73**, 413-418 (1989).
12. X. Wang, O. Sasaki, T. Suzuki, and T. Maruyama, "Response characteristics of a self-pumped phase-conjugate mirror to spatially nonuniform phase changes of an incident wave and their applications," *Opt. Eng.* **34**, 1184-1190 (1995).
13. X. Wang, O. Sasaki, T. Suzuki, and T. Maruyama, "Measurement of spatially nonuniform phase changes of a light beam utilizing reflectivity characteristic of a self-pumped phase-conjugate mirror," *Opt. Eng.* **38**, 1553-1559 (1999).
14. O. Sasaki and H. Okazaki, "Sinusoidal phase modulating interferometry for surface profile measurement," *Appl. Opt.* **25**, 3137-3140 (1986).